Materials Letters 273 (2020) 127919

Contents lists available at ScienceDirect

Materials Letters

journal homepage: www.elsevier.com/locate/mlblue

# Divulging the electrochemical hydrogen storage on nitrogen doped graphene and its superior capacitive performance

Sivagaami Sundari Gunasekaran [a], Thileep Kumar Kumaresan [a], Shanmugaraj Andikkadu Masilamani [b], Smagul Zh. Karazhanov [c], Kalaivani Raman [a], Raghu Subashchandrabose [b,*]

[a] Department of Chemistry, Vels Institute of Science, Technology & Advanced Studies (VISTAS), Chennai 600 117, Tamil Nadu, India
[b] Centre for Advanced Research & Development (CARD),/Chemistry, Vels Institute of Science, Technology & Advanced Studies (VISTAS), Chennai 600 117, Tamil Nadu, India
[c] Institute for Energy Technology, P.O Box 40, NO 2027-Kjeller, Norway

ARTICLE INFO

*Article history:*
Received 13 April 2020
Received in revised form 28 April 2020
Accepted 30 April 2020
Available online 4 May 2020

*Keywords:*
Nitrogen doped graphene
Hydrogen storage
Electrochemical mechanism
Capacitance

ABSTRACT

Capacitive energy storage is one of the electrochemical energy storage systems with a short charging moment giving power density. The electrochemical aqueous hydrogen storage capability of graphene and functionalized graphene with the study of structural, capacitive and faradaic energy contribution is explored specifically at the earliest. The functionalized (nitrogen) graphene shows excellent electrochemical hydrogen storage. The graphene and nitrogen functionalized graphene showed discharge capacity of 52 mAh $g^{-1}$ and 38 mAh $g^{-1}$ and maximum specific capacitance of 273 F $g^{-1}$ and 374 F $g^{-1}$. Understanding the contribution can provide suggestions for building high capacitance, specific energy and power of energy storage devices.

© 2020 Elsevier B.V. All rights reserved.

## 1. Introduction

The most promising contenders to replace the present carbon-based energy services is hydrogen, a pollution-free energy, which could be generated from renewable energy resources [1,2]. Typical storage of hydrogen was concerned with storing hydrogen gas in confined form, metal hydride or by high surface adsorption chemisorption [3]. There is a significant effort to test and store hydrogen in the light elements like carbon/graphene-based materials to reduce the weight density issues [4,5]. Graphene is a robust flexible membrane, which can be modified or functionalized to promote future Nano science, energy storage/conversion and hydrogen storage applications [6]. Storing hydrogen ($H^+$ ions) electrochemically is an effective technique where adsorption of hydrogen takes place during the deposition in the aqueous electrolyte, but have comparatively small ability and requires enhancement in the storage capability [7,8]. The electrochemical hydrogen storage of pristine graphene (GR) and nitrogen-doped graphene (NGR) and their hydrogen-storing mechanism is investigated in this study [9].

## 2. Experimental section

A mixture of cyanamide and GO (Hummer's Method) [10] solution was made under stirring and heating at 90 °C until dry and was shifted into Teflon lined autoclave at 400 °C for 1 day and then calcined at 900 °C, evolving to nitrogen-doped graphene (NGR) [11]. The electrode material was fabricated by mixing with 85% active material, 10% of conducting carbon and 5% of Teflon solution with Iso-ethanol/propyl alcohol solvent. The solution was homogenously mixed until it becomes a paste and made into film and dried at 120 °C in the vacuum oven [12].

## 3. Results and discussions

The FTIR spectra (Agilent Technology Cary 600 Series) (Fig. 1a) of GR and NGR shows the in-plane stretching peaks at 1728 $cm^{-1}$ (C=O), 1629 $cm^{-1}$ (C=C), 1363 $cm^{-1}$ (O–H) and 1225 $cm^{-1}$ (C–O), representing the GO formation and 2135 $cm^{-1}$ (C=C), 1614 $cm^{-1}$ (N–H), 1442 $cm^{-1}$ (N–H),1363 $cm^{-1}$ (O–H) and 1218 $cm^{-1}$ (C–O), representing the nitrogen functionalized graphene. The XRD pattern (Bruker D8) (Fig. 1b) shows sharp peak at 22.9° (GR) and 26.8° (NGR) corroborating (0 0 2) plane. The calculated d-spacing-crystallite size ($L_c$)-disorderness degree (R) of GR and NGR is 0.33 nm, 1.8, 11.18 and 0.388 nm, 1.7, 3.14.

The Raman spectra (Jobin Yvon T64000) of GR and NGR (Fig. 1c) shows two prominent peaks of D and G band at 1379 $cm^{-1}$, 1602

* Corresponding author.
*E-mail addresses:* rakvani@yahoo.co.in (K. Raman), subraghu_0612@yahoo.co.in (R. Subashchandrabose).

https://doi.org/10.1016/j.matlet.2020.127919
0167-577X/© 2020 Elsevier B.V. All rights reserved.

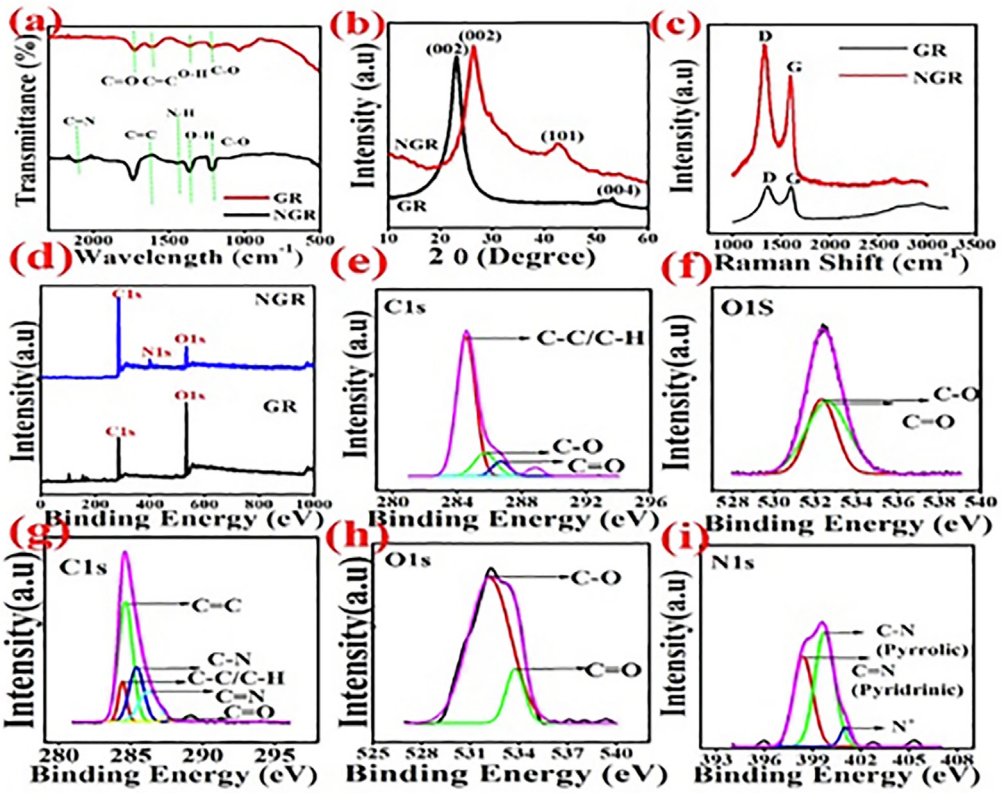


**Fig. 1.** (a) FTIR spectra, (b) XRD pattern, (c) Raman spectra, (d–i) XPS of GR and NGR.

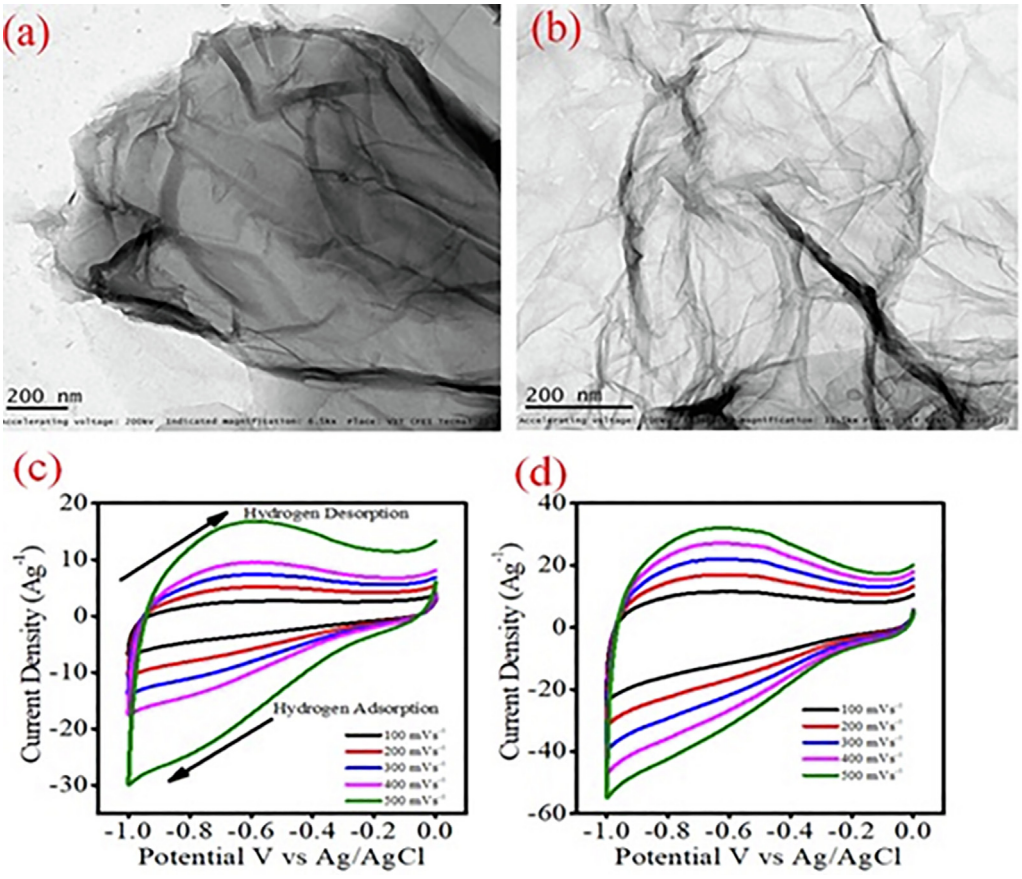


**Fig. 2.** (a, b) TEM images, (c, d) CV curve at different scan rates of GR and NGR.

$cm^{-1}$ and 1316 $cm^{-1}$, 1586 $cm^{-1}$. Due to the structural distortion, NGR has lower G band value. The $I_d/I_g$ values were found to be 0.86 (GR) and 1.3 (NGR), which corresponds to higher the dis-orderness, higher the $I_d/I_g$ Value [13]. The X-ray photon spectroscopy survey scan of GR and NGR (Fig. 1d) shows two peaks 284.5 eV, 530 eV corresponding to C1s and O1s and an addition peak at 400 eV corresponding to N1s with C1s and O1s. The atomic composition of carbon, oxygen and nitrogen at the surface level of GR and NGR are observed to be 0.6, 0.4 and 0.1, 0.8, 0.1. The number of oxygen atoms per 1000 carbon atoms was calculated and it is noted to be 377 atoms (GR) and 94 atoms (NGR) with ~108 nitrogen atoms was observed. From Fig. 1(e–i) De-convoluted C1s spectra of GR and NGR showed characteristic peaks of 284.6 eV, 286 eV and 287 eV representing the in-plane stretching of C–C/C–H, C–O and C═O; 284.1 eV, 284.6 eV, 285.5 eV, 286.5 eV and 287.2 eV corresponding to C═C, C–C, C–N/C–O, C═N, C═O. C. This fact is further supported by the de-convoluted O1s (C═O) and (C–O) spectra, at 532.2 eV 533.6 eV (GR) and 532.5 eV, 533 eV (NGR). The de-convoluted N1s spectra of NGR showed peaks of pyrrolic (C–N) 398.3 eV, pyridinic (C–N) 399.7 eV, which has more intensity and (C═N) and $N^+$ quaternary 400.9 eV [13]. Fig. 2(a, b) shows TEM images (JEM2100) at 200 nm, rough, less wrinkle (GR) and exfoliated nano-platelets with crumble-paper like (NGR) morphology observed [14]. Fig. 2 (c, d) depicted the CV (SP300 Biologic) behaviour of GR and NGR (6 M KOH electrolyte) at different scan rates and rectangular voltammetry characteristics can be observed. As the sweep rate increases, the current density is also increased. The maximum current density of 13 $Ag^{-1}$ (GR) and 20 $Ag^{-1}$ (NGR) observed. The specific capacitance of GR and NGR was found to be ~273 F $g^{-1}$ and ~374 F $g^{-1}$. From the CV results (Fig. 3(a–c)), the reduction peak is found at −0.96 V (cathode) and the oxidation peak between −0.78 and −0.85 (anode) which corresponds to the hydrogen storage. The proposed mechanism hydrogen storage is as follows; [15].

$$C_xH_yN_wO_z + H_2O \iff C_xH_yN_wO_z\text{-}H_{\text{adsorption}} + OH^- \quad (1)$$

$$C_xH_yN_wO_z\text{-}H_{\text{adsorption}} \iff C_xH_yN_wO_z\text{-}H_{\text{absorption}} \quad (2)$$

$$C_xH_yN_wO_z\text{-}H_{\text{absorption}} \rightarrow 2\ C_xH_yN_wO_z + H_2 \quad (3)$$

NGR has higher intensity of peak than GR, corresponding to superior property. The total capacitive contribution can be calculated using Eq. (4).

$$i(v) = k1\,v + k2\,v^{1/2} \quad (4)$$

where i is the CV curve intensity, $v$ is the scan rate, k1 and k2 are independent constants. $k1\,v$, the amount of capacitive performance which has pure capacitive performance including EDLC and redox and $k2\,v^{1/2}$, the amount of faradaic process.

This difference of current is depicted in Fig. 3(b, c) and it was found that NGR (374 F $g^{-1}$) has higher redox property than GR (273 F $g^{-1}$) corresponding to increased hydrogen storage. GCD

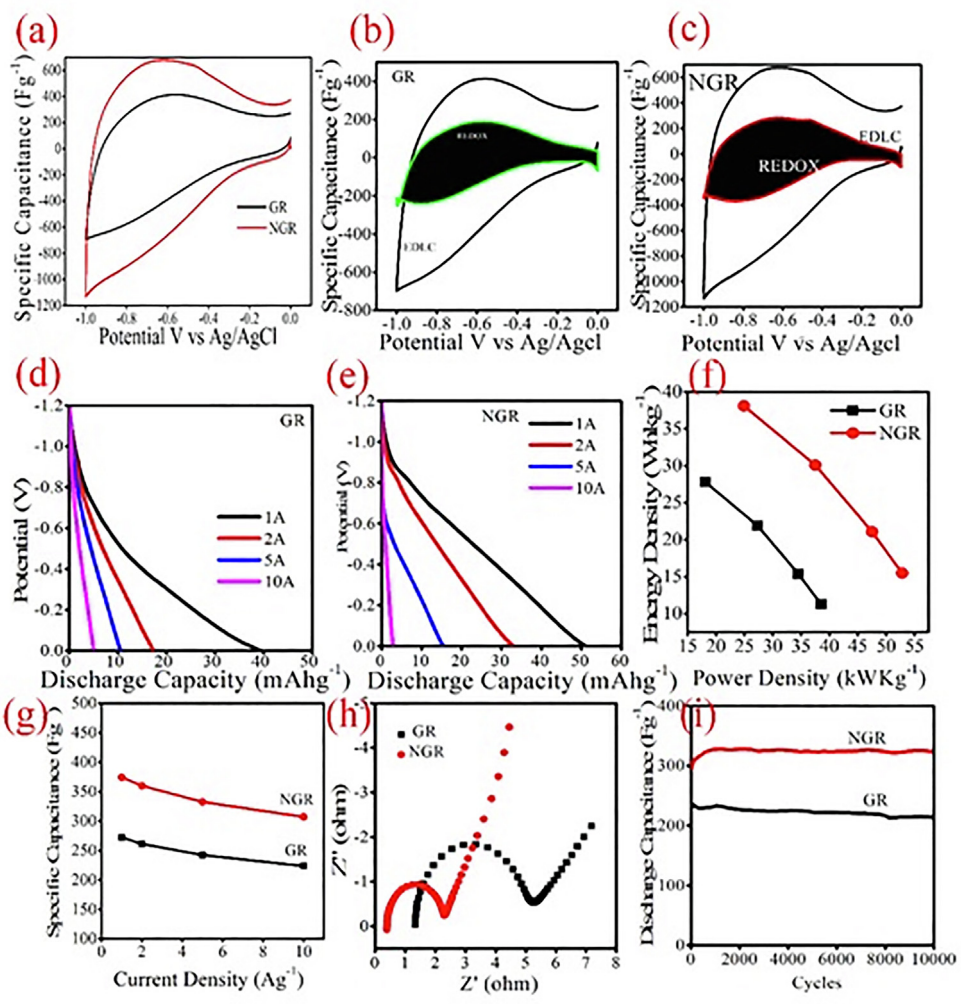


**Fig. 3.** (a) CV curve, (b, c) Redox behaviour at 20 mV $s^{-1}$, (d, e) GCD study, (f) Ragone's plot, (g) Rate performance, (h) EIS spectra, (i) cycling studies of GR and NGR.

studies (Neware Battery Tester) reveals a discharge capacity of 38 mAh $g^{-1}$ (GR) and 52 mAh $g^{-1}$ (NGR). The GR and NGR has the maximum half-cell specific capacitance, energy and power of 272.5 F $g^{-1}$, 27.8 Wh $kg^{-1}$, 38.5 kW $kg^{-1}$ and 374.4 F $g^{-1}$, 38.1 Wh $kg^{-1}$, 52.8 kW $kg^{-1}$. The NGR has the maximum specific energy of at 1 A $g^{-1}$ and specific power of 52.8 kW $kg^{-1}$ at 10 A $g^{-1}$, respectively. NGR has 37% increases in all the electrochemical parameters. Ragone's plot (Fig. 3f) and the rate performance graph (Fig. 3g) follows linear suitable trend. Impedance carried out between 0.001 kHz and 100 kHz shows spectrum of the NGR (Fig. 3h) a smaller semicircle at high frequency range which corresponds to the smaller charge-transfer resistance representing higher mobility of ions suitable for supercapacitor applications.

The calculated $R_s$ value for GR and NGR is 0.43 Ω and 0.40 Ω. The calculated $R_{ct}$ for GR and NGR are 5 Ω and 2 Ω, which is smaller than the former. The cyclic performances of the GR and NGR were carried out at 1 A $g^{-1}$ in the for 10,000 cycles. GR electrode has the decrease in capacitance till 500 cycles, and after that there follows the stability of the capacitance. Alternatively, up-to 1000 cycles, there is slight deterioration in the stability of NGR, and then follows the capacitance stability. The NGR and GR have the stability retention of 98% and 92% at the end of 10,000 cycles and it is shown in Fig. 3(f).

## 4. Conclusion

The prepared NGR with the enhanced electrochemical hydrogen storage confirms the maximum specific capacitance of 374.4 F $g^{-1}$ and 272.5 F $g^{-1}$ for the pure graphene. The peak representing the hydrogen storage is seen −0.7 V to −0.9 V. The maximum specific energy of NGR obtained is 38.1 Wh $kg^{-1}$ and specific power is 52.8 kW $kg^{-1}$ with 37% increase, that indicates that NGR is accountable for the improved electrochemical hydrogen storage.

## Declaration of Competing Interest

The authors declare that they have no known competing financial interests or personal relationships that could have appeared to influence the work reported in this paper.

## Acknowledgements

We gratefully acknowledge the financial support from (DST/TMD/MES/2K17/39), New Delhi and VISTAS. Sivagaami Sundari Gunasekaran is gratefully acknowledges the financial support from VISTAS, Grant Vels Research Fellowship (VRF).

## References

[1] X. Chen, Y. Zhang, X.P. Gao, G.L. Pan, X.Y. Jiang, J.Q. Qu, F. Wu, J. Yan, D.Y. Song, Int. J. Hydrogen Energy 29 (2004) 743–748, https://doi.org/10.1016/j.ijhydene.2003.08.010.
[2] T.K. Kumaresan, S.S. Gunasekaran, S.K. Elumalai, et al., Int. J. Hydrogen Energy 44 (2019) 25918–25929, https://doi.org/10.1016/j.ijhydene.2019.08.044.
[3] B. Fang, H. Zhou, I. Honma, J. Phys. Chem. B 110 (2006) 4875–4880, https://doi.org/10.1021/jp056063r.
[4] N. Rajalakshmi, K.S. Dhathathreyan, A. Govindaraj, B.C. Satishkumar, Electrochim. Acta 45 (2000) 4511–4515, https://doi.org/10.1016/S0013-4686(00)00510-7.
[5] K.T. Kumar, G.S. Sundari, E.S. Kumar, et al., Mater. Lett. 218 (2018) 181–184, https://doi.org/10.1016/j.matlet.2018.02.017.
[6] Z. Wen, X. Wang, S. Mao, Z. Bo, H. Kim, S. Cui, J. Chen, J. Adv. Mater. 24 (2012) 5610–5616, https://doi.org/10.1002/adma.201201920.
[7] X. Qin, X.P. Gao, H. Liu, H.T. Yuan, D.Y. Yan, W.L. Gong, D.Y. Song, Electrochem. Solid-State Lett. 3 (2000) 532–535, https://doi.org/10.1149/1.1391200.
[8] P. Chen, J.J. Yang, S.S. Li, Z. Wang, T.Y. Xiao, Y.H. Qian, S.H. Yu, Nano Energy 2 (2013) 249–256, https://doi.org/10.1016/j.nanoen.2012.09.003.
[9] I.H. Lin, Y.J. Tong, H.J. Hsieh, H.W. Huang, H.T. Chen, Int. J. Energy Res. 40 (2016) 230–240, https://doi.org/10.1002/er.3457.
[10] L. Shahriary, A.A. Athawale, Int. J. Renew. Energy Environ. Eng. 2 (2014) 58–63, https://doi.org/10.1016/j.proeng.2017.04.118.
[11] L. Sun, L. Wang, C. Tian, T. Tan, Y. Xie, K. Shi, et al., RSC Adv. 2 (2012) 4498–4506, https://doi.org/10.1039/C2RA01367C.
[12] S.S. Gunasekaran, S.K. Elumalali, T.K. Kumaresan, et al., Mater. Lett. 218 (2018) 165–168, https://doi.org/10.1016/j.matlet.2018.01.172.
[13] L.S. Panchakarla, K.S. Subrahmanyam, S.K. Saha, A. Govindaraj, H.R. Krishnamurthy, et al., Adv. Mater. 21 (2009) 4726–4730, https://doi.org/10.1002/adma.200901285.
[14] Y. Su, Y. Zhang, X. Zhuang, S. Li, D. Wu, et al., Carbon 62 (2013) 296–301, https://doi.org/10.1016/j.carbon.2013.05.067.
[15] S.S. Gunasekaran, R.S. Bose, K. Raman, Orient. J. Chem. 35 (2019) 302–307, https://doi.org/10.13005/ojc/350136.